

## ISM BAND RECTENNA USING A RING LOADED MONOPOLE

G. Monti\*, L. Corchia, and L. Tarricone

Innovation Engineering Department, University of Salento, Via per Monteroni, Lecce 73100, Italy

**Abstract**—This paper proposes a rectifying antenna (rectenna) for operation in the ISM (Industrial, Scientific and Medical) band centered at 2.45 GHz. It consists of a modified circular monopole loaded with a rectangular ring and a half-wave rectifier. Numerical and experimental data are reported and discussed. From measurements, it is demonstrated that when the power density incident on the monopole is  $155 \mu\text{W}/\text{cm}^2$ , the device here presented exhibits values of the RF-to-DC conversion efficiency higher than 30% in the frequency range 2.35–2.5 GHz with a maximum of about 50% at 2.45 GHz.

### 1. INTRODUCTION

In the last years a great attention has been paid to the possibility of harvesting the electromagnetic (EM) energy associated to wireless communication systems [1–5]. To this regard, the key component is a rectifying antenna (rectenna) [1–11], which consists of an antenna and a rectifier. The antenna plays the role of the EM harvester, it acts as a transducer between a free propagating EM wave and a guided one; while, the rectifier converts the energy collected by the antenna into a DC signal.

Most of the strategies for the design of efficient rectennas that have been proposed in the literature focus on the harvesting of the EM energy associated to wireless devices operating in the ISM band (see Table 1).

Among these, in [6] a system consisting of two parallel connected rectennas each one made out of a microstrip patch antenna and a dual-diode rectifier is presented. An RF-to-DC conversion efficiency of 60% with an input power of 10 mW is demonstrated.

---

*Received 28 August 2012, Accepted 19 September 2012, Scheduled 26 September 2012*

\* Corresponding author: Giuseppina Monti (giuseppina.monti@unisalento.it).

A 2.45 GHz bi-layer rectenna using a compact dual circularly polarized patch antenna is proposed in [7]. The measured conversion efficiency is of about 63% for a power density incident on the antenna of  $525 \mu\text{W}/\text{cm}^2$ .

In [8] a rectenna consisting of a second iteration Koch antenna and a two-stage Dickson charge pump voltage-doubler rectifier is proposed. A conversion efficiency of 70% for an input power of about 3 dBm is demonstrated for the rectifier.

In [9], two nested microstrip-fed shorted annular ring-slot antennas and two rectifier circuits are used to obtain a dual-frequency rectenna for wireless power transmission at 2.45 GHz and at 5.8 GHz. In the case of an input power of 0 dBm, the authors demonstrate a conversion efficiency of 55% at 2.45 and of 19 % at 5.8 GHz.

In order to obtain compact dimensions, a square aperture coupled patch antenna with a cross shaped slot is used in [10]; a conversion

**Table 1.** Summary of the main properties of the antennas analyzed in Section 1.

Refer.	Operating frequency [GHz]	Effic. [%]	RF Inp. Power to the rectifier [mW]	Inc. power Density [ $\mu\text{W}/\text{cm}^2$ ]	Main feature
[6]	2.45	60	10	/	<i>The input low-pass filter is not necessary</i>
[7]	2.45	63	/	525	<i>-Dual Circular polarization -Two output ports</i>
[8]	2.4	70	2	/	<i>Compactness</i>
[9]	2.45	55	1	/	<i>Dual frequency operation</i>
	5.8	19	1	/	
[10]	2.45	42	0.1	/	<i>-Compactness -Dual-linear polarization</i>
<i>Proposed antenna</i>	2.45	50	/	155	<i>-Compactness -Operation at low-input power</i>

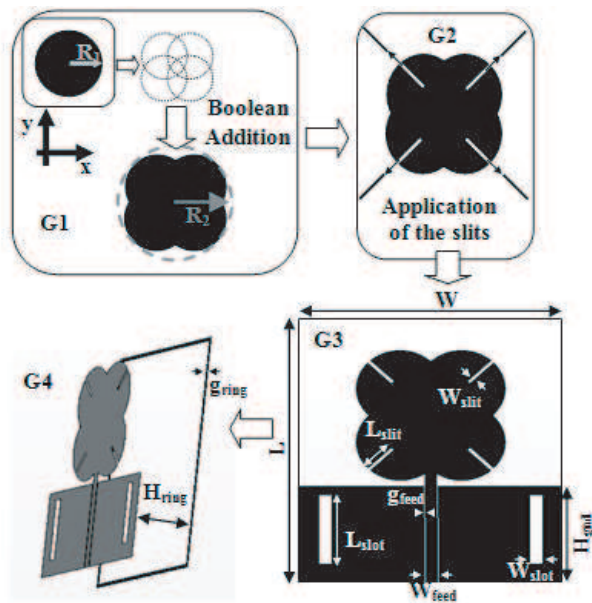
efficiency of about 42% is obtained with an input power level of  $-10$  dBm.

In this paper, a rectenna using a novel broadband monopole antenna and a half-wave rectifier is presented. Experimental data demonstrating a conversion efficiency of about 50% with an incident power density of  $155 \mu\text{W}/\text{cm}^2$  are reported and discussed.

## 2. ANTENNA DESIGN

The layout of the antenna used to collect the EM energy is illustrated in Fig. 1; it consists of a multi-layer structure that comprises a monopole antenna with a coplanar waveguide (CPW) feeding line [12–14] and a rectangular ring both realized on a FR4 single-sided copper clad laminate ( $\epsilon_r = 3.9$ ,  $\tan(\delta) = 0.019$ , thickness = 1.6 mm) and separated by a 15 mm-thick layer of air. In order to verify the performance corresponding to this design strategy, a first prototype of the antenna was developed to work without the rectifier and to be matched with respect to a  $50 \Omega$  impedance.

The steps of the antenna design process are illustrated in Fig. 1. We firstly optimized the geometry of the monopole and its feeding

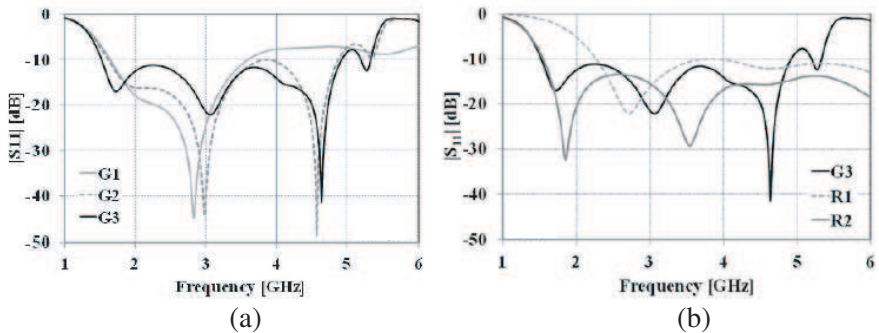


**Figure 1.** Geometry of the monopole antenna proposed in this paper.

**Table 2.** Dimensions of the final geometry of the monopole antenna.

$R_1$	$R_2$	$H_{\text{gnd}}$	$W_{\text{slit}}$	$L_{\text{slit}}$	$W_{\text{slot}}$
10	20	25.1	0.8	7.63	3

$L_{\text{slot}}$	$W_{\text{feed}}$	$g_{\text{feed}}$	$W$	$L$	$H_{\text{ring}}$	$g_{\text{ring}}$
18	2.6	0.3	60	68.5	15	1

**Figure 2.** (a) Numerical data calculated for the reflection coefficients corresponding to the geometries  $G_1$ ,  $G_2$  and  $G_3$ . (b) Comparison among the reflection coefficient corresponding to geometry  $G_3$  and the ones corresponding to two circular monopoles of radius  $R_1$  and  $R_2$ , respectively.

line by means of full-wave simulations performed with CST Microwave Studio [15] and with proprietary tools [16–20]. The starting point was the geometry  $G_1$  obtained by a boolean addition of four circular monopoles, then four slits was introduced along the boundary of  $G_1$  resulting in the geometry  $G_2$ . Finally, geometry  $G_3$  was achieved by designing two symmetrical slots on the ground plane; corresponding dimensions are given in Table 2.

The reflection coefficients corresponding to  $G_1$ ,  $G_2$  and to the final geometry  $G_3$  are compared in Fig. 2(a); it can be seen that both the introduction of the slits along the boundary of  $G_1$  and of the slots on the ground plane of  $G_2$ , result in an improvement of the antenna relative bandwidth. More specifically, from numerical data the relative bandwidth obtained for the three geometries corresponding to the monopole design steps are: 74% ( $G_1$ ), 100% ( $G_2$ ) and 111% ( $G_3$ ).

As for the performance of the proposed monopole with respect to a simple circular monopole, Fig. 2(b) shows a comparison with the reflection coefficients obtained for two circular monopoles of radius  $R_1$

and  $R_2$  (see Fig. 1), respectively. It can be noticed that, differently from a simple circular monopole that has a high-pass behavior, the proposed monopole exhibits a pass-band behavior. This pass-band behavior is useful in rectenna applications where it guarantees that the high-order harmonics generated by the rectifier will not be re-radiated by the antenna.

The final step of the antenna design process was the addition to the radiating element of a rectangular ring parallel to the antenna plane and placed at a distance  $d$  (see Fig. 1) that was optimized by means of full-wave simulations

The addition of this ring allows to modify the monopole radiation pattern; more specifically, it results in an increase of the gain of the antenna in the forward direction. This is highlighted in Fig. 3, where the three dimensional radiation pattern calculated at 2.45 GHz for the proposed monopole with and without the square ring is reported.

In order to verify the performance of the monopole antenna calculated by means of full-wave simulations, a prototype was realized and tested; photographs are given in Fig. 4(a). Measurements of the reflection coefficient were performed by means of the R&S® ZVL6 vector network analyzer and by using a Time Domain Reflectometry approach [21–25]; results obtained this way were in a perfect agreement. Fig. 4(b) compares the measured reflection coefficient with numerical data. From measurements the proposed monopole exhibits a relative impedance bandwidth of 136% ( $S_{11} < -10$  dB in the frequency range 1.03–5.41 GHz).

As for the gain, experimental data are illustrated in Fig. 5; at 2.45 GHz a maximum of 2 dB was measured.

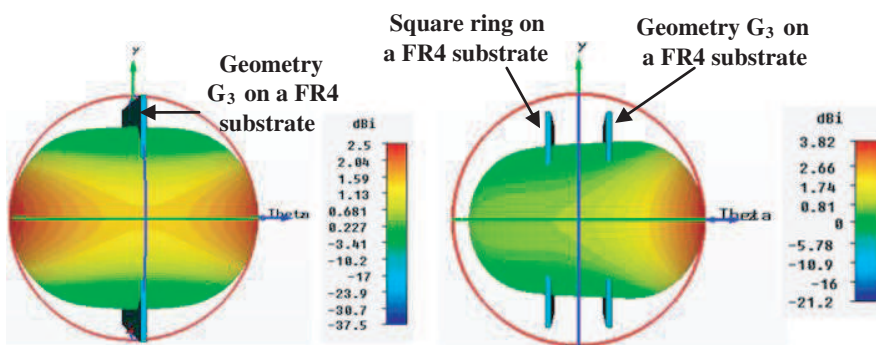


**Figure 3.** Three dimensional radiation pattern calculated at 2.45 GHz for the proposed monopole antenna with and without the square ring.

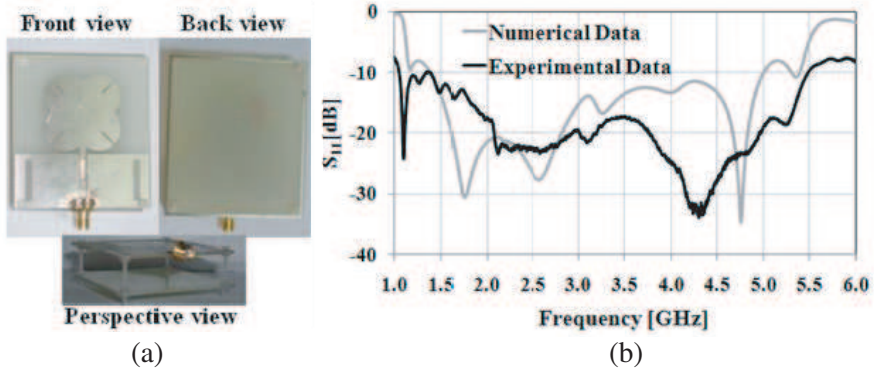


**Figure 4.** (a) Photographs of the realized monopole antenna. (b) Comparison between experimental and numerical data obtained for the prototype of the monopole antenna.

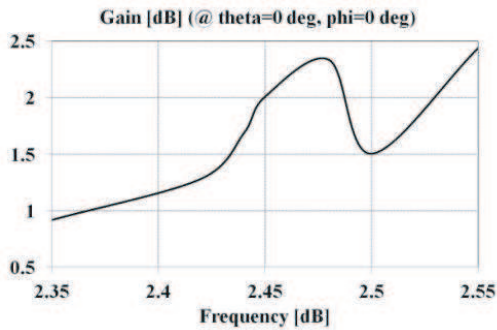


**Figure 5.** Experimental data obtained for the antenna gain.

### 3. RECTENNA DESIGN AND RESULTS ON CONVERSION EFFICIENCY

The layout of the rectenna proposed in this paper is illustrated in Fig. 6, it consists of the monopole antenna described in the previous section integrated with a rectifier. More specifically, a schematic representation of the circuit used for rectification is given in Fig. 7, it is a single diode half-wave rectifier.

A network consisting of two lumped inductors (ATC 0603 WL series wire wound chip [26]) was used for matching the rectifier to the monopole antenna. From Fig. 7, the presence, with respect to the resistive load, of a shunt lumped capacitor [27] and of a series schottky diode [28] can be also noticed. The capacitor acts as a low-pass filter

thus guaranteeing that only the DC signal is delivered to the load. While, the series diode was used to compensate temperature effects, thus resulting in an improvement of the rectifier performance [29].

The rectenna layout and the value of the lumped elements were optimized by combining full-wave and circuitual simulations.

More specifically, optimizations were performed to maximize the rectenna RF-to-DC conversion efficiency ( $\eta$ ) in the case of a resistive load of  $1000\ \Omega$  and for a power density incident on the monopole antenna of about  $100\ \mu\text{W}/\text{cm}^2$ . The optimum value calculated this way for the parameters of the layout illustrated in Fig. 6 are given in Table 3; the rectenna occupies a volume of about  $(60 \times 77.8 \times 18.2)\ \text{mm}^3$ . Photographs of a prototype are given in Fig. 8.

Experimental tests of the RF-to-DC conversion efficiency were performed by using a Software-Defined Radio (SDR) platform [2–4, 30–35]. More specifically the Universal Software Radio Peripheral (USRP) equipped with the XCVR2450 daughterboard [36] and a monopole antenna was used to generate the microwave signal incident on the monopole. The use of this setup was validated by the authors through

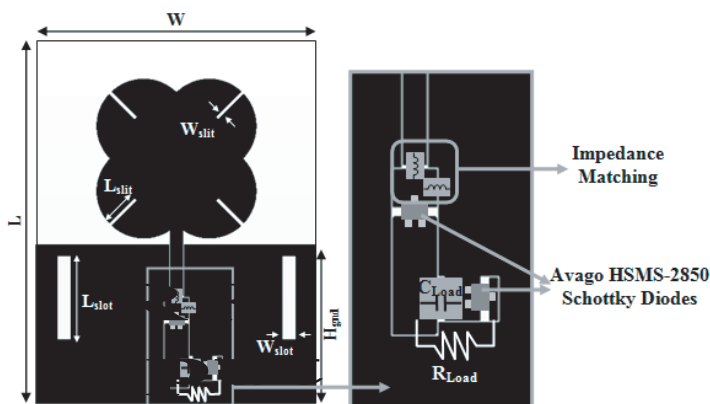
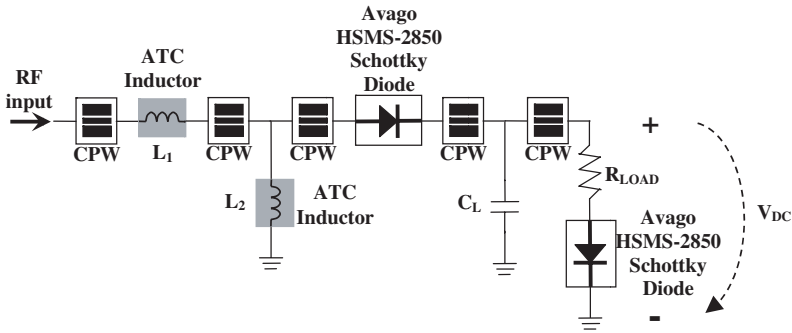


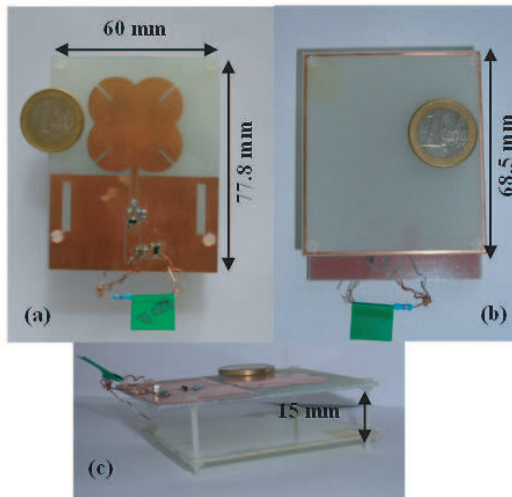
Figure 6. Layout of the proposed rectenna.

Table 3. Parameters of the proposed rectenna.

Layout dimensions (mm)						
$H_{\text{gnd}}$	$W_{\text{slit}}$	$L_{\text{slit}}$	$W_{\text{slot}}$	$L_{\text{slot}}$	$W$	$L$
34.4	0.8	7.63	3	18	60	77.8
Value of the lumped elements						
$L_1$	$L_2$	$C_1$	$R_L$			
3.9 nH	9.5 nH	4.7 $\mu\text{F}$	1000 $\Omega$			



**Figure 7.** Schematic representation of the circuit used for rectification.



**Figure 8.** Photographs of the realized rectenna. (a) Front-view. (b) Back-view. (c) Side-view.

the characterization of several antennas and systems [37–47].

In order to avoid spurious reflections and to guarantee that both antennas were operating in their far-field region, measurements were performed in a large outdoor area and by placing the USRP transmitting dipole at a distance of 50 cm from the rectenna.

A first set of experiments was performed for different values of the resistive load and of the power density of the microwave signal incident on the antenna. The following definition was used to calculate the RF-

to-DC conversion efficiency:

$$\eta = \frac{P_{OUT,DC}}{S_{RF}A_G} = \left( \frac{V_{DC}^2}{R_{LOAD}} \right) \frac{1}{S_{RF}A_{EFF}} \quad (1)$$

where  $S_{RF}$  is the power density incident on the antenna,  $V_{DC}$  is the DC output voltage (see Fig. 7),  $R_{LOAD}$  is the resistive load.  $A_{eff}$  is the monopole antenna effective area that was experimentally estimated as the ratio between the power received by the antenna and the incident power density:

$$A_{eff} = \frac{P_{RIC,RF}}{S_{RF}} = \left( \frac{\lambda_0^2 G}{4\pi} \right) \quad (2)$$

The PMM 8053A broadband field meter with the EP-183 isotropic probe was used to measure  $S_{RF}$ . Results obtained this way are given in Fig. 9. Fig. 9(a) illustrates the measured RF-to-DC conversion efficiency as function of the power density incident on the monopole antenna for different values of the resistive load; while, Fig. 9(b) shows the measured values of  $\eta$  as function of the resistive load. It can be seen that a maximum of 45% was measured for a resistive load of 820  $\Omega$  and for an incident power density of 155  $\mu W/cm^2$ . Fig. 10(a) shows the measured values of the output voltage used to calculate the conversion efficiency illustrated in Fig. 9(a).

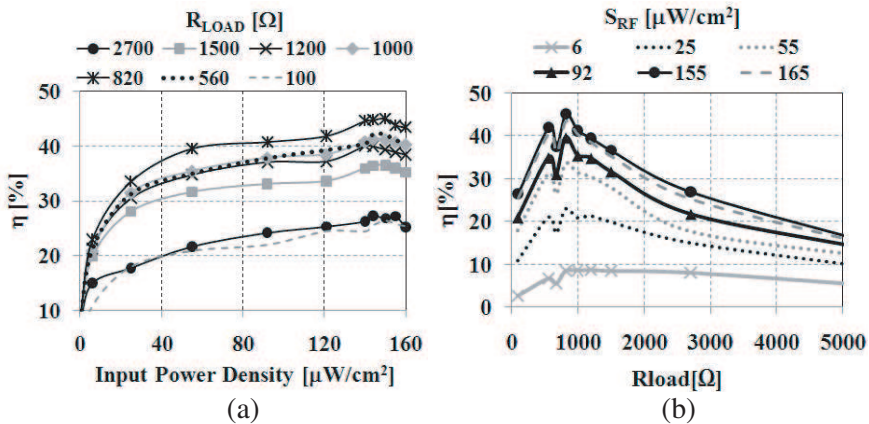


**Figure 9.** Experimental data obtained at 2.45 GHz for the conversion efficiency of the proposed rectenna. (a) Conversion efficiency as function of the power density incident on the antenna for different values of the resistive load. (b) Conversion efficiency as function of the resistive load for different values of the power density incident on the antenna.

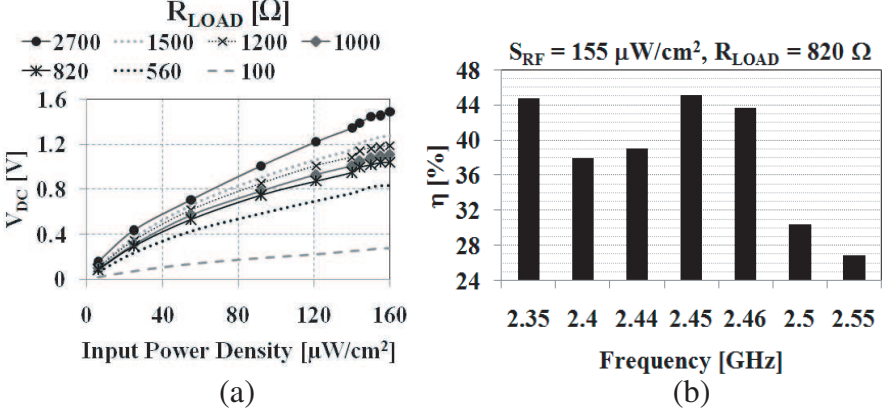


**Figure 10.** (a) Measured output voltage corresponding to the conversion efficiency illustrated in Fig. 9(a). (b) Measurements of the conversion efficiency performed by varying the frequency of the signal incident on the antenna.

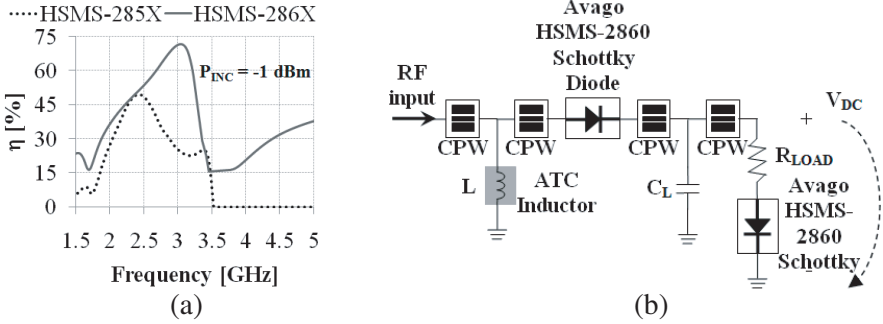


**Figure 11.** (a) Circuitual simulation results of the conversion efficiency. (b) Schematic of the rectifier designed by using the HSMS-2860 diode.

Calculations of the conversion efficiency as function of the frequency were also performed by varying the frequency of the signal generated by the USRP in the operating frequency range centered at 2.45 GHz (i.e., 2.35–2.55 GHz) of the XCVR2450 daughterboard. More specifically, experimental data were collected by varying the frequency of the microwave signal incident on the antenna while maintaining constant  $R_{LOAD}$  and  $S_{RF}$  at 820  $\Omega$  and 155  $\mu\text{W}/\text{cm}^2$ , respectively. Results obtained this way are summarized in Fig. 10(b), the proposed rectenna exhibits a conversion efficiency higher than 25% in the frequency range 2.35–2.55 MHz.

In order to investigate the performance of the proposed rectenna

over the entire bandwidth of the monopole presented in the previous section, circuital simulations were performed. In these simulations the antenna was taken into account in terms of input impedance by using results obtained by means of full-wave simulations. More specifically, in circuital simulations the impedance of the input port of the rectifier was the one numerically calculated for the antenna. Corresponding results are given in Fig. 11(a); it can be noticed that the conversion efficiency of the rectifier shown in Figs. 7 and 8 drops down drastically for frequencies above 3.5 GHz.

This is due to the use of the HSMS-2850 diode, which was the only one available in our laboratory. In fact, this diode is not well-suited to work at high-frequency; as a consequence improved results could be obtained for the RF-to-DC conversion efficiency by using a different diode. This has been confirmed by circuital simulations performed by using the HSMS-2860 diode. Fig. 11(b) shows the circuit schematic of the rectifier optimized for operation with the HSMS-286X; in Fig. 11(a) results obtained for the conversion efficiency are given and compared with the one corresponding to the HSMS-2850. It can be noticed that values of the conversion efficiency higher than 15% were calculated for frequencies above 3.5 GHz.

#### 4. CONCLUSION

A 2.45 GHz rectenna consisting of a novel compact monopole and a single diode rectifier has been presented. Experimental data referring both to the monopole antenna when designed to be matched to a  $50\ \Omega$  impedance and when used as a rectenna for energy harvesting applications are reported and discussed. It is demonstrated that the antenna here presented exhibits a relative bandwidth of 136%. As for the rectenna, from experimental data the RF-to-DC conversion efficiency is of about 50% when the power density incident on the monopole antenna is  $155\ \mu\text{W}/\text{cm}^2$ .

#### ACKNOWLEDGMENT

This work has been realized in the framework of the project “Nano-Rectenna for high Efficiency Direct Conversion of Sunlight to Electricity” funded by Regione Puglia.

#### REFERENCES

1. Takhedmit, H., B. Merabet, L. Cirio, B. Allard, F. Costa, C. Vollaïre, and O. Picon, “A 2.45-GHz low cost and efficient

- rectenna,” *Proc. 4th Europ. Conf. on Antenn. and Propag., EuCAP 2010*, Barcelona, Spain, 2010.
2. Monti, G., F. Congedo, D. De Donno, and L. Tarricone, “Monopole-based rectenna for microwave energy harvesting of UHF RFID systems,” *Progress In Electromagnetics Research C*, Vol. 31, 109–121, 2012.
  3. Congedo, F., G. Monti, L. Tarricone, and M. Cannarile, “Broad-band bowtie antenna for RF energy scavenging applications,” *Proc. 5th European Conf. on Antennas and Propag., EUCAP 2011*, 335–337, Rome, Italy, 2011.
  4. Monti, G. and F. Congedo, “UHF rectenna using a bowtie antenna,” *Progress In Electromagnetics Research C*, Vol. 26, 181–192, 2012.
  5. Riviere, S., F. Alicalapa, A. Douyere, and J.-D. Lan. Sun. Luk, “A compact rectenna device at low power level,” *Progress In Electromagnetics Research C*, Vol. 16, 137–146, 2010.
  6. Takhedmit, H., B. Merabet, L. Cirio, B. Allard, F. Costa, C. Vollaire, and O. Picon, “2.45-GHz dual-diode RF-to-DC rectifier for rectenna applications,” *Intern. Journ. of Microw. and Wireless Techn.*, Vol. 3, 251–258, 2011.
  7. Harouni, Z., L. Cirio, L. Osman, A. Gharsallah, and O. Picon, “A dual circularly polarized 2.45-GHz rectenna for wireless power transmission,” *IEEE Antenn. and Wirel. Propag. Lett.*, Vol. 10, 306–309, 2011.
  8. Olgun, U., C.-C. Chen, and J. L. Volakis, “Low-profile planar rectenna for batteryless RFID sensors,” *Proc. IEEE Intern. Symp. on Antenn. and Propag., APSURSI 2010*, Toronto, Canada, 2010.
  9. Heikkinen, J. and M. Kivikoski, “A novel dual-frequency circularly polarized rectenna,” *IEEE Antenn. Wireless Propag. Lett.*, Vol. 2, 330–333, 2003.
  10. Andia Vera, G., A. Georgiadis, A. Collado, and S. Via, “Design of a 2.45 GHz rectenna for electromagnetic (EM) energy scavenging,” *Proc. IEEE Radio and Wireless Symp., RWS 2010*, 61–64, Barcelona, Spain, 2010.
  11. Monti, G., L. Tarricone, and M. Spartano, “X-band planar rectenna,” *IEEE Antenn. and Wireless Propag. Lett.*, Vol. 10, 1116–1119, 2011.
  12. Monti, G., L. Corchia, L. Tarricone, T. Idda, F. Coccetti, and R. Plana, “Broadband compact planar monopole,” *Microwave and Optical Technology Letters*, Vol. 53, No. 12, 2838–2842, 2011.
  13. De Paolis, R., G. Monti, L. Tarricone, and M. V. De Paolis,

- “A compact coplanar-fed monopole for broadband applications,” *Proc. 5th Europ. Conf. on Antenn. and Propag., EuCAP 2011*, 354–356, 2011.
14. Monti, G., L. Corchia, L. Valentino, and L. Tarricone, “Compact planar monopole for broad band applications,” *Proc. 4th Europ. Conf. on Antenn. and Propag., EUCAP 2010*, 2010.
  15. <http://www.cst.com/>.
  16. De Donno, D., A. Esposito, G. Monti, and L. Tarricone, “Iterative solution of linear systems in electromagnetics (and not only): Experiences with CUDA,” *Lecture Notes in Computer Science (Including Subseries Lecture Notes in Artificial Intelligence and Lecture Notes in Bioinformatics)*, 6586 LNCS, 329–337, 2011.
  17. De Donno, D., A. Esposito, G. Monti, and L. Tarricone, “Efficient acceleration of sparse MPIE/MoM with graphics processing units,” *Proc. — 41st European Microw. Conf., European Microw. Week 2011: “Wave to the Future”*, 175–178, 2011.
  18. De Donno, D., A. Esposito, G. Monti, and L. Tarricone, “GPU-based acceleration of MPIE/MoM matrix calculation for the analysis of microstrip circuits,” *Proc. 5th European Conf. on Antennas and Propag., EUCAP 2011*, 3921–3924, 2011.
  19. De Donno, D., A. Esposito, G. Monti, and L. Tarricone, “Parallel efficient method of moments exploiting graphics processing units,” *Microw. and Optical Techn. Lett.*, Vol. 52, No. 11, 2568–2572, 2010.
  20. Catarinucci, L., G. Monti, and L. Tarricone, “A parallel-grid-enabled variable-mesh FDTD approach for the analysis of slabs of double-negative metamaterials,” *IEEE Antenn. and Propag. Society, AP-S Intern. Symp. (Digest)*, 782–785, 2005.
  21. Cataldo, A., G. Monti, E. De Benedetto, G. Cannazza, L. Tarricone, and L. Catarinucci, “Assessment of a TD-based method for characterization of antennas,” *IEEE Transactions on Instrumentation and Measurement*, Vol. 58, No. 5, 1412–1419, May 2009.
  22. Cataldo, A., E. De Benedetto, G. Cannazza, and G. Monti, “A reliable low-cost method for accurate characterization of antennas in time domain,” *Metrology and Measurement Systems*, Vol. 15, No. 4, 571–583, 2008.
  23. Cataldo, A., G. Monti, E. De Benedetto, G. Cannazza, L. Tarricone, and L. Catarinucci, “A comparative analysis of reflectometry methods for characterization of antennas,” *Proc. IEEE Instrum. Meas. Technol. Conf.*, 240–243, 2008.

24. Cataldo, A., G. Monti, E. De Benedetto, G. Cannazza, and L. Tarricone, "A noninvasive resonance-based method for moisture content evaluation through microstrip antennas," *IEEE Transactions on Instrumentation and Measurement*, Vol. 58, No. 5, 1420–1426, 2009.
25. Cataldo, A., G. Monti, G. Cannazza, E. De Benedetto, L. Tarricone, L. M. Cipressa, "A non-invasive approach for moisture measurements through patch antennas," *Proc. of IEEE Instrumentation and Measurement Technology Conference*, 1012–1015, 2008.
26. <http://www.atceramics.com/>.
27. <http://www.murata.eu/>.
28. <http://www.avagotech.com/pages/home/>.
29. Mbombolo, S. E. F. and C. W. Park, "An improved detector topology for a rectenna," *Microw. Workshop Series on Innovat. Wireless Power Transmission: Technologies, Systems, and Applicat. (IMWS), IEEE MTT-S Intern.*, 23–26, May 12–13, 2011.
30. De Donno, D., F. Ricciato, L. Catarinucci, and L. Tarricone, "Design and applications of a software-defined listener for UHF RFID systems," *IEEE MTT-S International Microwave Symposium Digest*, Baltimore, MD, USA, June 2011.
31. De Donno, D., L. Tarricone, L. Catarinucci, V. Lakafosis, and M. M. Tentzeris, "Performance enhancement of the RFID epc gen2 protocol by exploiting collision recovery," *Progress In Electromagnetics Research B*, Vol. 43, 53–72, 2012.
32. Catarinucci, L., D. De Donno, M. Guadalupi, F. Ricciato, and L. Tarricone, "Performance analysis of passive UHF RFID tags with GNU-radio," *Proc. IEEE Intern. Symp. on Antennas and Propagation, APSURSI*, 541–544, Spokane, WA, 2011.
33. De Donno, D., L. Catarinucci, R. Colella, F. Ricciato, and L. Tarricone, "Differential RCS and sensitivity calculation of RFID tags with software-defined radio," *Proc. IEEE Radio and Wireless Symp., RWS*, 9–12, Santa Clara, CA, 2012.
34. Catarinucci, L., D. De Donno, R. Colella, F. Ricciato, and L. Tarricone, "A cost-effective SDR platform for performance characterization of RFID tags," *IEEE Transactions on Instrumentation and Measurement*, Vol. 61, No. 4, 903–911, 2012.
35. De Donno, D., F. Ricciato, L. Catarinucci, A. Coluccia, and L. Tarricone, "Challenge: Towards distributed RFID sensing with software-defined radio," *Proc. Annual International Conference*

- on Mobile Computing and Networking, MOBICOM*, 97–104, Chicago, IL, 2010.
36. Ettus Research LLC, <http://www.ettus.com>.
  37. Catarinucci, L., R. Colella, and L. Tarricone, “Design, development, and performance evaluation of a compact and long-range passive UHF RFID tag,” *Microw. and Optical Techn. Lett.*, Vol. 54, No. 5, 1335–1339, 2012.
  38. Catarinucci, L., R. Colella, and L. Tarricone, “A cost-effective UHF RFID tag for transmission of generic sensor data in wireless sensor networks,” *IEEE Trans. on Microw. Theory and Techniques*, Vol. 57, No. 5, 1291–1296, 2009.
  39. Monti, G., L. Catarinucci, and L. Tarricone, “Compact microstrip antenna for RFID applications,” *Progress In Electromagnetics Research Letters*, Vol. 8, 191–199, 2009.
  40. Monti, G., L. Catarinucci, and L. Tarricone, “Broad-band dipole for RFID applications,” *Progress In Electromagnetics Research C*, Vol. 12, 163–172, 2010.
  41. Congedo, F., G. Monti, and L. Tarricone, “Modified bowtie antenna for GPR applications,” *Proc. of the 13th International Conference on Ground Penetrating Radar, GPR 2010*, 2010.
  42. Monti, G., L. Corchia, and L. Tarricone, “Planar bowtie antenna with a reconfigurable radiation pattern,” *Progress In Electromagnetics Research C*, Vol. 28, 61–70, 2012.
  43. Monti, G., L. Catarinucci, and L. Tarricone, “Experimental validation of a plasma model for electromagnetic metal foam shields,” *IEEE MTT-S International Microwave Symposium Digest*, 145–148, 2009.
  44. Monti, G. and L. Tarricone, “Signal reshaping in a transmission line with negative group velocity behavior,” *Microw. and Optical Techn. Lett.*, Vol. 51, No. 11, 2627–2633, 2009.
  45. Monti, G. and L. Tarricone, “Negative group velocity in a split ring resonator-coupled microstrip line,” *Progress in Electromagnetics Research*, Vol. 94, 33–47, 2009.
  46. Monti, G., L. Catarinucci, and L. Tarricone, “Metal foams for electromagnetic shielding: A plasma model,” *Proc. of Europ. Conf. on Antenn. and Propag., EuCAP 2009*, 2123–2126, 2009.
  47. Monti, G. and L. Tarricone, “Dispersion analysis of a negative group velocity medium with MATLAB,” *Applied Comput. Electromagnet. Society Journ.*, Vol. 24, No. 5, 478–486, 2009.